



Determination of ascorbic acid using electrochemiluminescence sensor based on nitrogen and sulfur doping graphene quantum dots with luminol as internal standard

Pingkun Liu¹ · Hui Meng¹ · Qian Han¹ · Gui Zhang¹ · Cun Wang¹ · Li Song¹ · Yingzi Fu¹

Received: 19 August 2020 / Accepted: 16 February 2021 / Published online: 10 March 2021
© The Author(s), under exclusive licence to Springer-Verlag GmbH, AT part of Springer Nature 2021

Abstract

A novel internal standard electrochemiluminescence (ECL) sensor has been designed for the detection of ascorbic acid (AA). The adopted dual-emission luminophore (NSGQDs-PEI-luminol-Pt) is composed of nitrogen and sulfur double-doped graphene quantum dots (NSGQDs, as the main luminophore), luminol (as the auxiliary luminophore and internal standard), platinum nanoparticles (Pt NPs, as the co-reaction accelerator), and polyetherimide (PEI, as the linker of NSGQDs and luminol). The results suggest obviously enhanced ECL intensities by the Förster resonance energy transfer (FRET) between luminol (donor) and NSGQDs (acceptor). In this sensing system, the cathodic ECL intensities of NSGQDs (ECL-1, -1.8 V vs. Ag/AgCl) gradually decrease with increasing concentration of AA, while the anodic ECL intensities of luminol (ECL-2, 0.3 V vs. Ag/AgCl) almost remain essentially constant at a potential window from -2.0 to 0.4 V. The natural logarithm of the ratio between ECL-1 and ECL-2 ($\ln I_{(ECL-1/ECL-2)}$) shows a good linear relationship with AA concentration ranging from 10 to 360 nM. The regression equation is $\ln I_{(ECL-1/ECL-2)} = -0.0059 c_{AA} + 3.55$ ($R^2 = 0.992$) with a limit of detection of 3.3 nM. Such sensor has also been applied for monitoring AA in human serum. The recovery range was 96.5 – 105.3% and the relative standard deviation was 1.3 – 3.3% .

Keywords Electrochemiluminescence · Internal standard method · Graphene quantum dots · Ascorbic acid · Luminol

Introduction

Electrochemiluminescence (ECL) technology has become a powerful analytical tool due to the low cost, simple operation, fast analysis, and high sensitivity [1]. It is well known that the measurement accuracy and efficiency of ECL directly limit the wide application of ECL sensors. However, the self-annihilating ECL luminophore alone is unable to provide a high enough signal. Since $C_2O_4^{2-}$ was first reported as a co-reactant, it has become a fashion to construct a binary system of ECL luminophores and co-reacting reagents in order to obtain significantly enhanced ECL signals. Commonly used co-reaction reagents include hydrogen peroxide, persulfate,

and tripropylamine [2]. In addition, different methods have also been used to improve the ECL system, such as resonant energy transfer [3] and introduction of nanomaterials [4]. Förster resonance energy transfer (FRET) can improve the ECL intensity and stability of single luminescent material through energy transfer between donor and acceptor. Nanomaterials can play a variety of roles in ECL, for example, luminophores, co-reaction accelerators, and carriers.

Graphene quantum dots (GQDs), as a kind of novel zero-dimensional nanomaterials, possess some unique properties, such as low toxicity, excellent biocompatibility, good stability, and water solubility [5]. However, the primal GQDs without passivated surface often present low ECL efficiency [6]. Heteroatom doping is considered to be a valid method to tune the surface state, optical properties, and chemical features of GQDs [7]. For example, the electrochemical properties, surface chemical activity, and quantum yield are improved by sulfur or nitrogen doped GQDs [8, 9]. Therefore, GQDs doping with diverse elements are becoming a research topic.

To solve some potential systematic errors caused by single ECL technology and make the detection results more

✉ Yingzi Fu
fyzc@swu.edu.cn

¹ Key Laboratory of Luminescence Analysis and Molecular Sensing (Southwest University), Ministry of Education, School of Chemistry and Chemical Engineering, Southwest University, Chongqing 400715, China

convincing, the ratiometric ECL sensors with dual-emission signals have been introduced [10]. For example, a ratiometric ECL sensor based on CdS nanocrystal and luminol has been developed for mp53 oncogene detection [11], and a dual-wavelength ratiometric electrochemiluminescence resonance energy transfer aptasensor has been constructed for amyloid- β protein detection, which based on the carbon nitride nanosheet as the energy donor and metal-organic framework as the acceptor [12]. However, when the dual signals change simultaneously, the reference signal cannot express the real status of the ECL system, which makes the reproducibility of the assay doubtful. The internal standard method has been introduced as an indirect or relative calibration method to solve this problem [13], which has been widely used in chromatography [14], fluorescence (FL) [15], Raman spectroscopy [16], and photoelectrochemical sensing [17]. That is to say, one ECL signal of the system remains constant as an internal reference while the other ECL signal changes sensitively according to the target, which can not only effectively avoid potential interferences but also greatly improve the reproducibility.

The dosage of ascorbic acid (AA) in human serum can be used as an indicator of some chronic diseases. The average level of AA in serum for a large number of people is 0.2 mg per 100 mL [18]. A series of methods have been developed to detect AA, including high-performance liquid chromatography [19], electroanalysis [20], ECL and so on [21].

Inspired by the above research, we present a novel composite (NSGQDs-PEI-luminol-Pt) to construct an internal standard ECL sensor for the detection of AA. Here, nitrogen and sulfur double doped graphene quantum dots (NSGQDs) and luminol are integrated into one nanostructure as the dual-emission luminophore, NSGQDs as the main luminophore, luminol as the auxiliary luminophore and internal standard, platinum nanoparticles (Pt NPs) as a co-reaction accelerator, and polyetherimide (PEI) as a linker of NSGQDs and luminol. The stable ECL signals corresponding to NSGQDs and luminol have been observed at -2.0 V (ECL-1) and 0.4 V (ECL-2), respectively. With the increasing concentration of AA, the ECL-1 decreases gradually, whereas ECL-2 remains almost constant, which can be considered an internal standard calibration (Scheme 1). The internal standard ECL system can avoid the detection errors of the false positive or negative results generated by the single peak ECL. It will be a good choice for the detection of AA or other small molecules in organisms.

Experiment section

Reagents and materials

Ascorbic acid (AA, 99%), polyetherimide (PEI, 99%), and glutaric dialdehyde (GA, 50%), citric acid (99%), L-cysteine

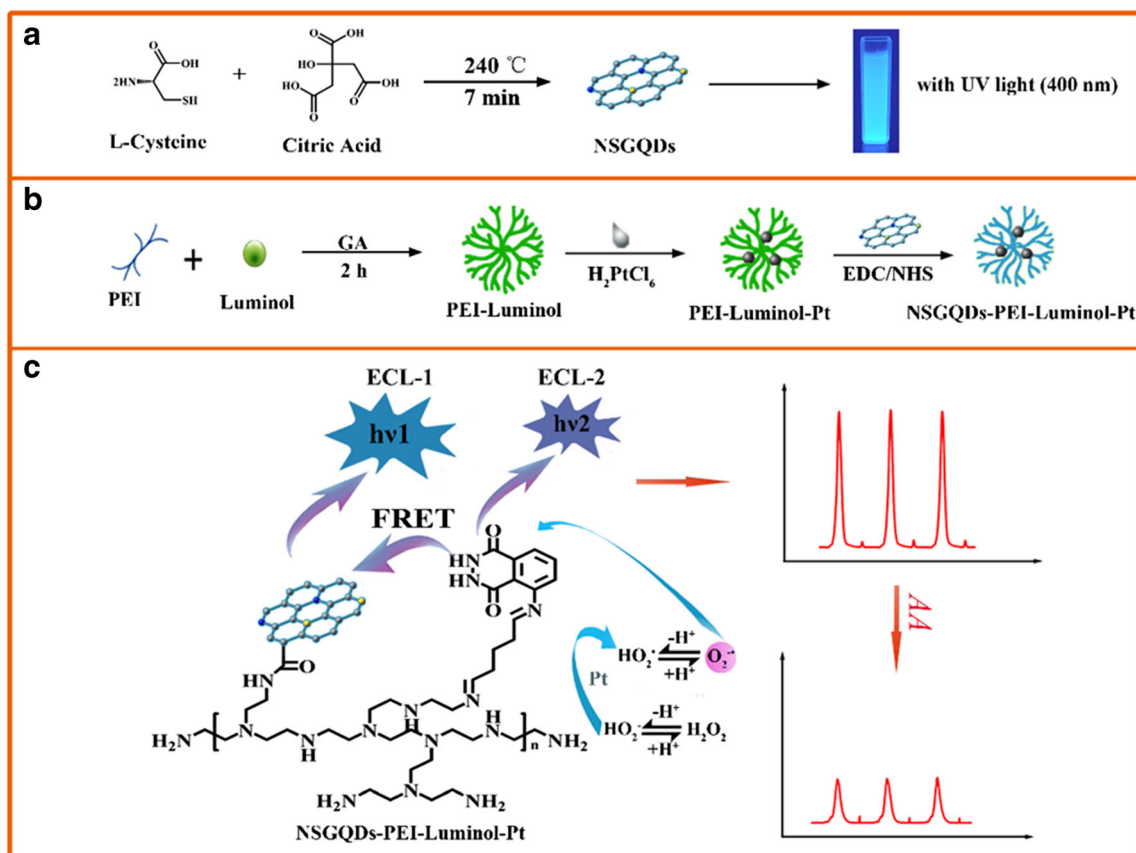
(97%), and chloroplatinic acid ($\text{H}_2\text{PtCl}_6 \cdot 6\text{H}_2\text{O}$, 99%) were got from Sigma-Aldrich Chem. Co. (St. Louis, MO, USA). N-Hydroxy succinimide (NHS, 99%) and N-(3-dimethylaminopropyl)-N'-ethylcarbodiimide hydrochloride (EDC, 99%) were acquired from J&k Chemical Co. (Beijing, China). 0.1 M phosphate buffer (PB, pH 7.4) was prepared by using 0.1 M Na_2HPO_4 and 0.1 M KH_2PO_4 containing 0.1 M KCl. 5.0 mM $[\text{Fe}(\text{CN})_6]^{4-/3-}$ solution (0.1 M PB, pH 7.4) was prepared by $\text{K}_4\text{Fe}(\text{CN})_6$ and $\text{K}_3\text{Fe}(\text{CN})_6$. Multi-walled carbon nanotubes (MWNTs, D = 40–60 nm) were purchased from Aladdin Reagent Co. Ltd. (Shanghai, China; www.aladdin-e.com). All chemicals were analytical grade and used as received without further purification. Ultrapure water (Millipore, 18.2 $\text{M}\Omega\cdot\text{cm}$) was used throughout this work.

Apparatus

Electrochemical determination was conducted on a CHI 660E electrochemical workstation (Shanghai Chenhua Instruments, China). ECL detection was performed using a model MPI-A electrochemiluminescence analyzer (Xi'an Remex Analysis Instruments Co. Ltd., China). The potential scanning range is from -2.0 to 0.4 V (vs. Ag/AgCl) and the photomultiplier tube was set at 600 V. A three-electrode system was employed: a glassy carbon electrode (GCE, $\Phi = 4.0$ mm) or modified GCE as working electrode, a platinum wire as counter electrode, and an Ag/AgCl electrode (saturated KCl) as reference electrode. The UV 2600 spectrometer (Shimadzu, Japan) was used to record the UV-vis spectra in the range from 200 to 800 nm. JEM-1200EX transmission electron microscopy (TEM) was applied to receive the morphology and structure of the materials at an accelerating voltage of 120 kV (JEOL, Japan). Scanning electron microscopy (SEM) images and energy-dispersive spectra (EDS) were acquired on a field-emission SEM (ZEISS, Germany). The X-ray photoelectron spectroscopy (XPS) analysis was obtained using a VG Scientific ESCALAB 250 spectrometer (Thermoelectricity Instruments, USA).

Preparation of the different composites

PEI-luminol-Pt PEI, an amino-rich polyelectrolyte, has been used as both a functional agent and a reductant with the assistance of formic acid to fabricate Pt NPs. First, PEI (4 mL, 0.05%), luminol (1.5 mL, 5 mM), GA (100 μL , 1%), and 5 mL of water were added into a 25-mL round-bottom flask and then stirred for 2 h at room temperature to make PEI and luminol cross-link sufficient. Next, H_2PtCl_6 solution (0.5 mL, 0.1 M) and 1 mL of formic acid were added into the above mixture. To accelerate the reaction, the above mixture was refluxed at 80 °C for 30 min (Scheme 1b).



Scheme 1 The preparation of (a) NSGQDs and (b) NSGQDs-PEI-luminol-Pt composite. (c) Possible ECL mechanism of NSGQDs-PEI-luminol-Pt system

NSGQDs-PEI-luminol-Pt The dual-emission luminophore was obtained as follows. First, NSGQDs were prepared according to the literature with slight modification (Scheme 1a) [22]. Then, 500 μL of NSGQDs was activated by EDC/NHS (v/v = 4:1) solution for 40 min at 4 $^\circ\text{C}$ and mixed with 1 mL of PEI-luminol-Pt, which shortens the distance of the donor-receptor pair and produces an enhanced ECL luminescence signal, resulting in a significant quenching of the ECL of NSGQDs improving the sensitivity of the sensor. The mixture was stirred for 12 h at 4 $^\circ\text{C}$. Last, the precipitates were collected by centrifugation and redispersed in 2 mL of water.

Fabrication of the ECL sensor

Prior to modification, each GCE was polished with 0.3 μm and 0.05 μm alumina respectively to achieve a mirror-like surface. Afterwards, 5 μL of MWCNTs dispersion was coated on the surface of the GCE and dried in air. Then, 10 μL NSGQDs-PEI-luminol-Pt was dropped on and dried in air (denoted as NSGQDs-PEI-luminol-Pt/MWCNTs/GCE). ECL analyses were executed in 0.1 M PB (pH 7.4) including 5 mM H_2O_2 and different concentrations of AA.

Results and discussion

Characterization of NSGQDs and NSGQDs-PEI-luminol-Pt

The morphologies of NSGQDs and NSGQDs-PEI-luminol-Pt composite were characterized by TEM and SEM, respectively. The NSGQDs show a spherical structure with the size around 1.5–5.5 nm (Fig. 1a). The high-resolution transmission electron microscope (HR-TEM) image exhibits that the lattice distance is 0.27 nm (Fig. 1b). The SEM image of the NSGQDs-PEI-luminol-Pt composite exhibits homogeneously flower-like shape with an average diameter of 1 μm (Fig. 1c). The element type and chemical state of NSGQDs-PEI-luminol-Pt composite were examined by XPS. As depicted in Fig. 1d, the characteristic peaks at 284.5, 399.9, and 532.5 eV belong to C 1s, N 1s, and O 1s respectively, and the peak at 72.5 eV belongs to Pt 4f. The results prove the presence of C, N, O, and Pt in NSGQDs-PEI-luminol-Pt composite. Additionally, the proposed composite was analyzed by HR-XPS spectra. As shown in Fig. 1e, the raw data of C 1s spectra can be fitted by three components of C-C (284.6 eV), C-N (285.7 eV), and O-C=O (288.6 eV). As depicted in Fig. 1f, two peaks at 399.8 and 402.1 eV correspond to C-NH₂ and

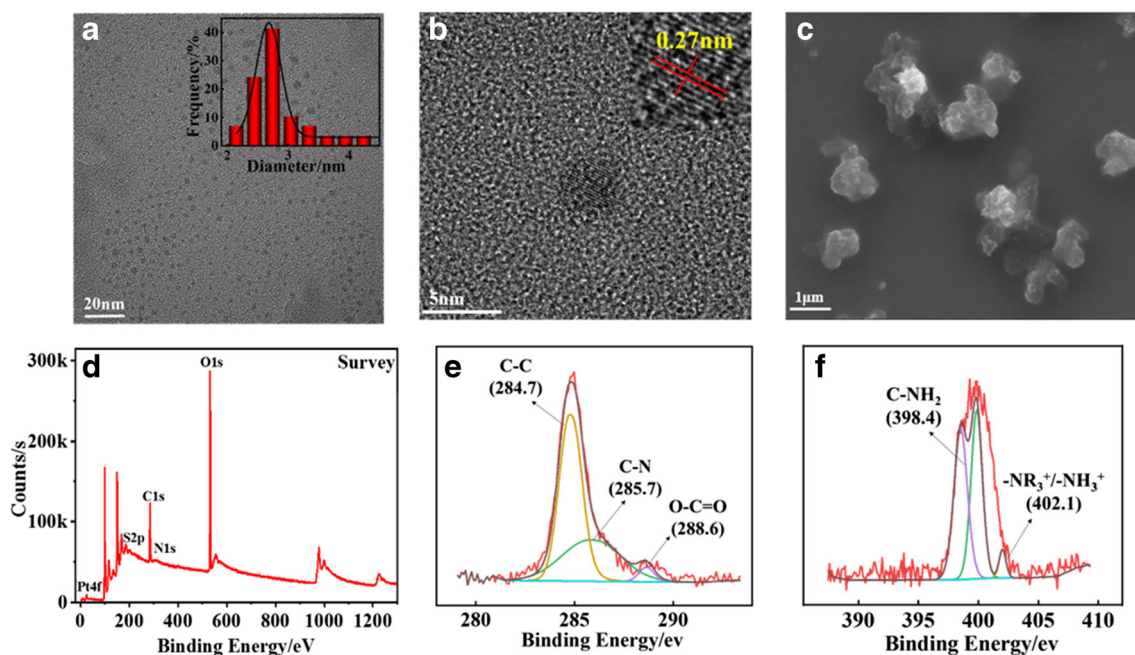


Fig. 1 (a) TEM and (b) HR-TEM images of the NSGQDs, (c) SEM image of the NSGQDs-PEI-luminol-Pt, (d) XPS analysis for the full region, and HR-XPS spectra of (e) C 1s and (f) N 1s of NSGQDs-PEI-luminol-Pt

-NR₃⁺/-NH₃⁺ respectively in high-resolution N 1s spectra. The above characterization indicates the successful preparation of NSGQDs-PEI-luminol-Pt composite.

Optical and electrical properties

The optical and electrical properties of the NSGQDs-PEI-luminol-Pt were also investigated via FL and ECL. As shown in Fig. 2A, a significant spectral overlap is observed from the FL emission spectrum of luminol (curve a) and the excitation spectrum of NSGQDs (curve b), indicating that the FRET between luminol (donor) and NSGQDs (acceptor) is possible. In other words, the NSGQDs can receive energy from luminol and can be excited to generate luminescence signal subsequently [23]. As shown in Fig. 2B, two ECL peaks are observed from NSGQDs-PEI-luminol-Pt, suggesting luminol and NSGQDs are co-existed in this dual-emission luminophore. The shoulder ECL peak located at 425 nm (ECL-2) is assigned to luminol, while the maximum ECL emission located at 484 nm (ECL-1) is raised from NSGQDs.

Furthermore, the ECL behaviors of luminol, PEI, NSGQDs, NSGQDs-PEI-luminol, and NSGQDs-PEI-luminol-Pt were studied comparatively at the potential window of -2.0 to 0.4 V (Fig. 3A). A small anodic ECL peak (0.4 V) is observed from luminol in 0.1 M PB (pH 7.4) containing 5 mM H₂O₂ as a co-reactant (curve a), while almost no obvious signal is detected in PEI solution (curve b). A weak cathodic ECL signal is obtained on NSGQDs (curve c), as well as a weak cathodic ECL signal and an anodic ECL signal are displayed on NSGQDs-PEI-luminol (curve d). Interestingly, a very high cathodic peak (ECL-1, -1.8 V, main emission from NSGQDs) accompanied by a weak anodic peak (ECL-2, 0.3 V, auxiliary emission from luminol) is appeared on NSGQDs-PEI-luminol-Pt (curve e). Compared with NSGQDs-PEI-luminol, dependent on the dual-emission luminophore NSGQDs-PEI-luminol-Pt, the ECL-1 is improved. Due to the presence of Pt NPs, the reaction between luminol and H₂O₂ was accelerated and further enhanced ECL-1 via FRET.

Fig. 2 (A) FL (a) emission spectrum for luminol and (b) excitation spectrum for NSGQDs. (B) ECL spectrum of NSGQDs-PEI-luminol-Pt

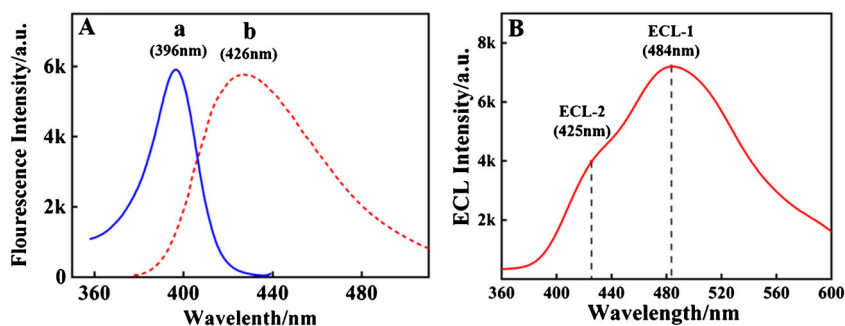
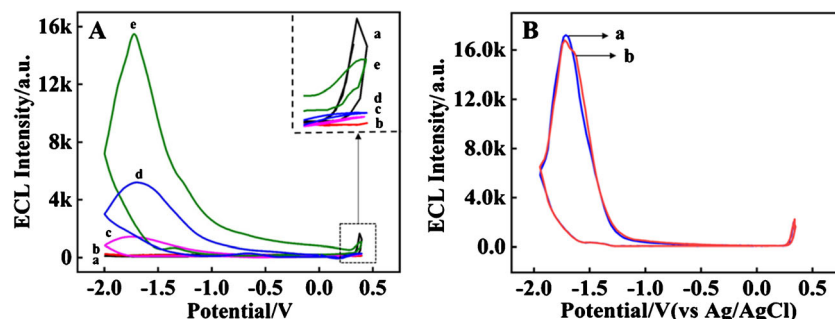


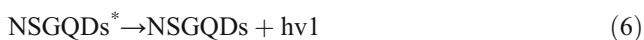
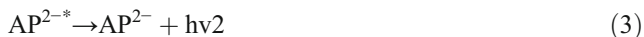
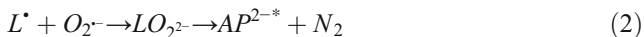
Fig. 3 (A) ECL profiles of (a) luminol, (b) PEI, (c) NSGQDs, (d) NSGQDs-PEI-luminol, and (e) NSGQDs-PEI-luminol-Pt in 0.1 M PB containing 5 mM H₂O₂. (B) Before (a) and after (b) purging high-purity nitrogen in NSGQDs-PEI-luminol-Pt system



The effect of dissolved O₂ to the ECL response has been investigated by comparing the signals before and after deaeration (Fig. 3B). No obvious change in ECL peak position and intensity has been observed, indicating that dissolved oxygen in solution has little effect on ECL reaction process.

ECL mechanism of NSGQDs-PEI-luminol-Pt

The possible ECL mechanism of the NSGQDs-PEI-luminol-Pt system is proposed (Scheme 1C). Since NSGQDs and luminol are integrated into one nanostructure, which can be oxidized synchronously on the surface of GCE. After the electrochemical oxidation, luminol anions (LH⁻) and NSGQDs are converted into luminol radicals (L^{•-}) [24] and NSGQDs cations (NSGQDs⁺), respectively. Superoxide radical (O₂^{•-}) are produced by decomposition of H₂O₂. Afterwards, L^{•-} reacts with O₂^{•-} to generate the excited state 3-aminophthalate (AP^{2-*}). Next, AP^{2-*} releases energy by giving an ECL emission at 425 nm (*hν*₂) which can be absorbed by NSGQDs⁺ with a emission at 484 nm (*hν*₁) based on the FRET between luminol and NSGQDs. Owing to the co-existence of luminol (donor) and NSGQDs (acceptor) is shortened, which makes FRET easy to realize. At the same time, Pt NPs have excellent catalytic performance which can accelerate the production of O₂^{•-} from H₂O₂. The corresponding ECL route is proposed as follows:



Measurement of AA

Under the optimal experimental conditions (Fig. S6), the ECL-1 decrease with the increasing AA concentration from 10 nM to 360 nM, while the ECL-2 as internal standard signal

almost remain unchanged (Fig. 4A). The calibration plot was constructed by the natural logarithm of the ratio between ECL-1 and ECL-2 ($\ln I_{(ECL-1/ECL-2)}$) and the concentration of AA (Fig. 4B). The linear equation of this ECL system is $\ln I_{(ECL-1/ECL-2)} = -0.0059 c_{AA} + 3.55$ ($R^2 = 0.992$) with a limit of detection (LOD) of 3.3 nM ($S/N = 3$). Compared with the previous method, the proposed sensor can detect AA with higher sensitivity and wider linear range (Table 1), but it is disposable.

Stability and selectivity of the ECL sensor

The stability of the present internal standard ECL sensor has been evaluated by the consecutive cyclic potential for 200 s in different AA concentrations (0.1 M PB containing 5 mM H₂O₂, pH 7.4) (Fig. 5a, Fig. S7). As depicted in Fig. 5a, the relative standard deviations (RSD) of ECL-1 and ECL-2 are 0.58% and 1.8% in 60 nM AA, indicating that reversibility and reliability of the system meet the regular requirements. The selectivity of the internal standard ECL system toward different interferences was investigated using various biologically relevant co-existing species including amino acid molecules of cysteine (Cys), phenylalanine (Phe), and tryptophan (Trp); small biological molecules of creatinine (Cre), glucose (Glu), and globulins (Glb); and common inorganic ions such as K⁺, Na⁺, Ca²⁺, Fe²⁺, and Fe³⁺ (Fig. 5b). The concentration of interference substances is 100-fold (vs molecules) or even

Table 1 Comparison assay of different strategies for AA detection

Method	LOD (μM)	Linear range(μM)	Reference
Electrochemistry	7.71	15–800	[25]
Photoluminescence	1.25	3.33–400	[26]
Fluorescence	0.13	0.5–200	[27]
Fluorescence	0.3	1–750	[28]
luminescent	0.0043	0.03–0.22	[29]
colorimetric	0.3	1–110	[30]
Electrochemiluminescence	70	0.1–100	[31]
Electrochemiluminescence	0.0033	0.01–0.36	This work

Fig. 4 (A) ECL intensity against various concentration of AA under optimized conditions. (B) Linear calibration plot for AA detection from a to i: 0, 10, 60, 100, 120, 180, 220, 270, and 360 nM, respectively

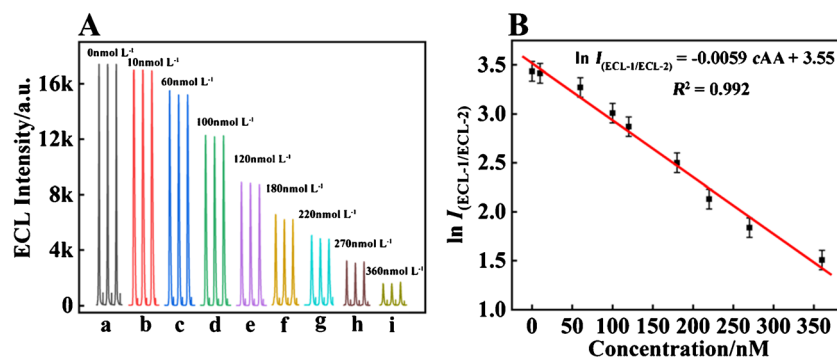
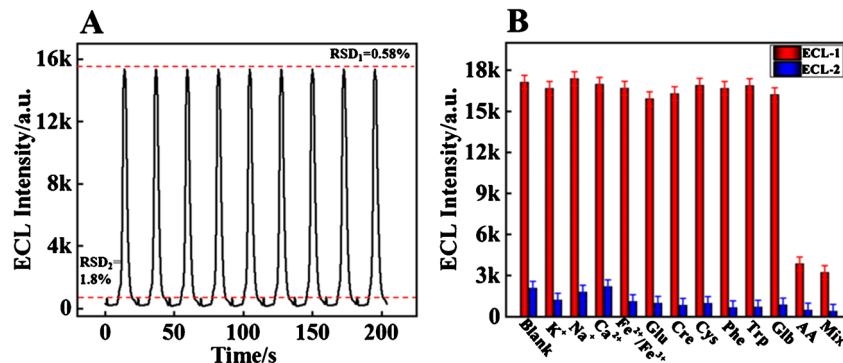


Fig. 5 (a) ECL stability of the sensor under consecutive cyclic potential for 200 s in 60 nM AA. (b) Selectivity evaluation of the sensor for AA (300 nM) and the interference molecules (30 μ M each) or interference ions (300 μ M each). Error bars: SD; $n = 3$



1000-fold (vs common inorganic ions) that of AA (300 nM). Compared with the target AA, the small changes of ECL intensity appear with the addition of the interference substances, whereas a significantly decreased intensity present when AA is added (Fig. 5b).

Real applicability

To investigate the applicability of this strategy in real practice, human serum samples were selected for assay using the standard addition method. Prior to use, the samples were diluted 100-fold with 0.1 M PB (pH = 7.4) and spiked with different concentrations of AA. Under the same conditions as the standard sample, the ECL analyses were executed in 3 mL sample solution including 5 mM H₂O₂ with the proposed sensor. The results are listed in Table 2, and the recovery rates are in the range of 96.5–105.3% with the RSD ranged from 1.3 to 3.3%,

Table 2 Recovery tests for AA in human serum

Sample	Added (nM)	Found (nM)	RSD (%) (n=3)	Recovery (%)
1	50	47.5	1.3	105.2
2	150	155.4	3.3	96.5
3	250	252.1	1.5	99.1

indicating that the proposed method can be effectively used for AA detection in real sample.

Conclusion

In this work, an internal standard ECL sensor was prepared based on NSGQDs-PEI-luminol-Pt composite as a novel luminophore for sensitive detection of AA. The proposed internal standard ECL sensor exhibits a strong cathodic ECL-1 signal and an almost constant anodic ECL-2 signal and an improved sensitivity and accuracy for the detection of AA, possibility of employment in other ECL system.

Supplementary Information The online version contains supplementary material available at <https://doi.org/10.1007/s00604-021-04761-w>.

Funding This work was supported by the National Natural Science Foundation of China (22077105) and Natural Science Foundation Project of CQ CSTC (cstc2020jcyj-msxmX0854), China.

Declarations

Conflict of interest The authors declare that they have no competing interests.

References

1. Valenti G, Zangheri M, Sansaloni SE, Mirasoli M, Penicaud A, Roda A, Paolucci F (2015) Transparent carbon nanotube network for efficient electrochemiluminescence devices. *Chem Eur J* 21: 12640–12645
2. Rubinstein I, Bard AJ (1981) Electrogenerated chemiluminescence. 37. Aqueous ecl systems based on tris(2,2'-bipyridine)ruthenium(2+) and oxalate or organic acids. *J Am Chem Soc* 103:512–516
3. Liu JL, Zhao M, Zhuo Y, Chai YQ, Yuan R (2017) Highly efficient intramolecular electrochemiluminescence energy transfer for ultra-sensitive bioanalysis of aflatoxin m1. *Chem Eur J* 23:1853–1859
4. Chen Y, Zhou S, Li L, Zhu JJ (2017) Nanomaterials-based sensitive electrochemiluminescence biosensing. *Nano Today* 12:98–115
5. Tetsuka H, Asahi R, Nagoya A, Okamoto K, Tajima I, Ohta R, Okamoto A (2012) Optically tunable amino-functionalized graphene quantum dots. *J Adv Mater* 24:5333–5338
6. Sun HJ, Gao N, Wu L, Ren JS, Wei WL, Qu XG (2013) Highly photoluminescent amino-functionalized graphene quantum dots used for sensing copper ions. *Chem Eur J* 19:13362–13368
7. Du Y, Guo SJ (2016) Chemically doped fluorescent carbon and graphene quantum dots for bioimaging, sensor, catalytic and photoelectronic applications. *Nanoscale* 8:2532–2543
8. Li S, Li Y, Cao J, Zhu J, Fan L, Li X (2014) Sulfur-doped graphene quantum dots as a novel fluorescent probe for highly selective and sensitive detection of Fe³⁺. *Anal Chem* 86:10201–10207
9. Riaz R, Ali M, Sahito IA, Arbab AA, Maiyalagan T, Anjum AS, Ko MJ, Jeong SH (2019) Self-assembled nitrogen-doped graphene quantum dots (N-GQDs) over graphene sheets for superb electro-photocatalytic activity. *Appl Surf Sci* 480:1035–1046
10. Chen HM, Zhang H, Yuan R, Chen SH (2017) Novel double-potential electrochemiluminescence ratiometric strategy in enzyme-based inhibition biosensing for sensitive detection of organophosphorus pesticides. *Anal Chem* 89:2823–2829
11. Zhang HR, Xu JJ, Chen HY (2013) Electrochemiluminescence ratiometry: a new approach to DNA biosensing. *Anal Chem* 85: 5321–5325
12. Wang Y, Zhang Y, Sha H, Xiong X, Jia N (2019) Design and biosensing of ratiometric electrochemiluminescence resonance energy transfer aptasensor between g-C₃N₄ nanosheet and Ru@MOF for amyloid-β protein. *ACS Appl Mater Inter* 11:36299–36306
13. Lin Y, Wang J, Luo F, Guo LH, Qiu B, Lin ZY (2018) Highly reproducible ratiometric aptasensor based on the ratio of amplified electrochemiluminescence signal and stable internal reference electrochemical signal. *Electrochim Acta* 283:798–805
14. Boysen A K, Heal K R, Carlson L T, Ingalls A E (2017) Best-matched internal standard normalization in liquid chromatography-mass spectrometry metabolomics applied to environmental samples. *Anal Chem* 1363–1369
15. Gong Q, Qin W, Xiao P, Wu X, Li L, Zhang G, Zhang R, Sun J, Yao SQ, Huang W (2020) Internal standard fluorogenic probe based on vibration-induced emission for visualizing PTP1B in living cells. *Chem Commun* 56:58–61
16. Shuang L, Xiang L, Yuan LL, Hai YZ, Wu LH, Li W (2018) Self-assembly of Au@Ag core-shell nanocubes embedded with internal standard for reliable quantitative SERS measurements. *Anal Methods-UK* 10:4201–4208
17. Dong YX, Cao JT, Wang B, Ma SH, Liu YM (2018) Spatial-resolved photoelectrochemical biosensing array based on a CdS@g-C₃N₄ heterojunction: a universal immunosensing platform for accurate detection. *ACS Appl Mater Inter* 10:3723–3731
18. Organization W H (1970) Requirements of ascorbic acid, vitamin D, vitamin B 12, folate, and iron: report of a joint FAO/WHO expert group. WHO
19. Bottegal M, Lang L, Miller M, McCord B (2010) Analysis of ascorbic acid based black powder substitutes by high-performance liquid chromatography/electrospray ionization quadrupole time-of-flight mass spectrometry. *Rapid Commun Mass Spectrom* 24: 1377–1386
20. Zare HR, Nasirizadeh N (2011) A comparison of the electrochemical and electroanalytical behavior of ascorbic acid, dopamine and uric acid at bare, activated and multi-wall carbon nanotubes modified glassy carbon electrodes. *J Iran Chem Soc* 8:S55–S66
21. Li XJ, Sun X, Fan DW, Yan T, Feng R, Wang H, Wu D, Wei Q (2019) A ternary quenching electrochemiluminescence insulin immunosensor based on Mn²⁺ released from MnO₂@Carbon core-shell nanospheres with ascorbic acid quenching AuPdPt-MoS₂@TiO₂ enhanced luminol. *Biosens Bioelectron* 142:111551
22. Zhang RZ, Adsetts JR, Nie YT, Sun XH, Ding ZF (2018) Electrochemiluminescence of nitrogen- and sulfur-doped graphene quantum dots. *Carbon* 129:45–53
23. Cao J, Zhang H, Liu X, Zhou N, Yang D (2019) Plasmon-coupled forster resonance energy transfer between silicon quantum dots. *J Phys Chem C* 123:23604–23609
24. Cui H, Zou GZ, Lin XQ (2003) Electrochemiluminescence of luminol in alkaline solution at a paraffin-impregnated graphite electrode. *Anal Chem* 75:324–331
25. Habibi B, Pourmaghi-Azar MH (2010) Simultaneous determination of ascorbic acid, dopamine and uric acid by use of a MWCNT modified carbon-ceramic electrode and differential pulse voltammetry. *Electrochim Acta* 55:5492–5498
26. Ma Q, Li Y, Lin ZH, Tang G, Su XG (2013) A novel ascorbic acid sensor based on the Fe³⁺/Fe²⁺ modulated photoluminescence of CdTe quantum dots@SiO₂ nanobeads. *Nanoscale* 5:9726–9731
27. Rong M, Lin L, Song X, Wang Y, Zhong Y, Yan J, Feng Y, Zeng X, Chen X (2015) Fluorescence sensing of chromium (VI) and ascorbic acid using graphitic carbon nitride nanosheets as a fluorescent “switch”. *Biosens Bioelectron* 68:210–217
28. Zhang Y, Fang X, Zhao H, Li Z (2018) A highly sensitive and selective detection of Cr (VI) and ascorbic acid based on nitrogen-doped carbon dots. *Talanta* 181:318–325
29. Wang YN, Wang SD, Yang LL, Zhao YF, Yang QF (2020) A luminescent cadmium coordination polymer for highly sensitive detection of ascorbic acid. *J Solid State Chem* 289:121519
30. Liu YH, Wei ZN, Duan WX, Ren CL, Jiang D (2018) A dual-mode sensor for colorimetric and “turn-on” fluorescent detection of ascorbic acid. *Dyes Pigments* 149:491–497
31. Chen H, Li W, Zhao P, Nie Z, Yao S (2015) A CdTe/CdS quantum dots amplified graphene quantum dots anodic electrochemiluminescence platform and the application for ascorbic acid detection in fruits. *Electrochim Acta* 178:407–413

Publisher's note Springer Nature remains neutral with regard to jurisdictional claims in published maps and institutional affiliations.